VDMA
Fluid Power Association

22nd ISC

International Sealing Conference

Stuttgart, Germany
October 01 - 02, 2024

Sealing Technology –
Challenges accepted!

IMA UNI STUTTGART

ISBN 978-3-8163-0768-6

Fachverband Fluidtechnik im VDMA e. V. Lyoner Str. 18
50628 Frankfurt am Main
Germany

Phone +49 69 6603-1513
E-Mail maximilian.baxmann@vdma.org
Internet www.vdma.org/fluid

Influence of hydrogen environment on friction properties of silicone rubber

Hikaru Hashimoto, Suguru Norikyo, Ayako Aoyagi, Hiroyoshi Tanaka, Takehiro Morita, Yoshinori Sawae, Joichi Sugimura

To elucidate the effect of hydrogen on the friction properties of silicone rubber, sliding tests were conducted in hydrogen and air with various moisture contents. The friction coefficient in hydrogen was higher than that in air. Regarding moisture content in hydrogen, the rubber surface after sliding test in humid hydrogen showed severe wear compared to that in dry hydrogen. These results suggested that gas atmosphere and moisture content of gas had influences on the friction between silicone rubber and austenitic stainless steel and the wear of silicone rubber. The surfaces of silicone rubber and austenitic stainless steel after sliding tests were analysed using optical microscopy, confocal laser scanning microscopy, FT-IR microscopy and SEM/EDS to explore the influence of hydrogen on the wear process.

1 Introduction

In recent years, the utilisation of hydrogen energy has gained importance in order to achieve carbon neutrality. Safe utilisation of hydrogen energy requires establishment of new technologies for ensuring reliability and durability of machine elements used in hydrogen networks, and the role of sealing materials is essential in achieving this goal. Examples of sealing elements used in high-pressure hydrogen gas applications include piston rings for reciprocating compressors and rubber O-rings for flanges, couplings and pressure vessels. Although O-rings are used as static seals for preventing gas leakage, they are subject to repeated micro-movements within the groove during compression-decompression cycles. Consequently, these O-rings experienced sliding against the metal groove surface in hydrogen gas. Especially, unexpected high friction of the O-ring causes excessive elastic deformation and possibly induces serious mechanical failure [1-12]. For these reasons, researches have intensively been conducted to understand frictional properties of rubber [13-17] and thermoplastics [18-21] in hydrogen.

In this study, the effect of hydrogen on friction between silicone rubber and stainless steel was investigated. Reciprocating sliding tests were performed with a pin-on-disk apparatus in air and hydrogen.

2 Experimental Methods

2.1 Material

Silicone rubber and austenitic stainless steel (AISI 316L steel) were selected as a representative material for O-rings and their metal sliding counterface, respectively, in high-pressure hydrogen gas applications. The silicone rubber pin specimen had a hemispherical shape with a diameter of 5 mm. The surfaces of the stainless steel disks were polished using 3 µm diamond slurry to have a surface roughness of 0.02 µm Ra. After that, the disks were cleaned ultrasonically using a mixture of acetone and hexane for three minutes.

2.2 Sliding test

Friction and wear of the silicone rubber-on-stainless steel sliding pair was evaluated by using a pin-on-disk apparatus installed in the vacuum chamber (*Figure 1 (a)*). The vacuum chamber was evacuated with a scroll and turbomolecular vacuum pumps. Then, the gas was introduced to raise the chamber to ambient pressure. The gas continued to flow in and out of the chamber during the sliding tests. Gas leaving the chamber was directed to a moisture sensor (HUMICAP®HM70, VAISALA). The gases were continued to flow during the sliding tests. Subsequently, load to press the rubber pin against the stainless steel disk was applied by dead weights through the loading lever. The applied load and friction force were measured using a biaxial load cell. Friction coefficients were calculated by friction force divided by load. Figure 1(b) shows the speed of stainless steel disk and the relative displacement of rubber pin to stainless steel disk during sliding test. The stainless steel disk rotated at a constant speed in a certain direction and quickly switched back to the other direction.

The purity of hydrogen was 99.999%. The vacuum chamber was equipped with a precision moisture controller which was developed by Fukuda [22] and used to adjust the trace moisture content of hydrogen gas environment. Several sliding tests were performed in hydrogen, which was moisturized by using this moisture controller. All sliding tests were performed for 10000 seconds. All experimental conditions are summarized in Table 1.

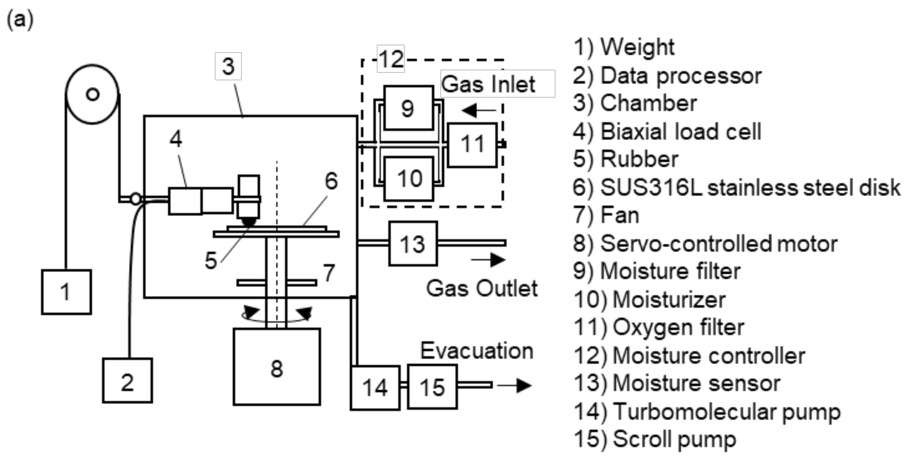

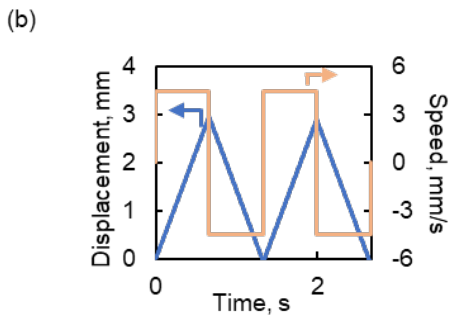

Figure 1: (a) Schematic diagram of pin-on-disk tribometer equipped with advanced atmosphere control system, (b) Motion of servo-controlled motor

Table 1: Conditions of sliding tests

Motion	Reciprocating sliding
Environment	Air, hydrogen
Load	5 N
Sliding speed	4.5 mm/s
Sliding distance	3 mm
Temperature	25 °C
Pressure	0.1 MPa

2.3 Surface analysis

2.3.1 Optical Microscopy and confocal laser microscopy

The worn surfaces of rubber specimens were observed by using optical microscope (VH7000, KENYENCE) at a magnification of 50. In addition to that, the specimens were observed by using a confocal laser microscope (VK-X1000, KENYENCE) at magnification of 10 to obtain 3D topography, arithmetic average roughness (Ra) and maximum roughness (Rz). The roughness parameters were measured on five positions near the top of rubber surface.

2.3.2 IR spectroscopy

Infrared (IR) spectroscopy (FT/IR 4X, IRT-7100, JASCO) was performed to collect spectra from silicone rubber and stainless steel. The IR spectra of silicone rubber confirming the wave number range of 400 to 4000 cm^{-1} were obtained by using attenuated total reflection (ATR) method with a diamond prism. The spectra from stainless steel surfaces were obtained by reflection method. The aperture size was 50 × 50 μm and the number of scans was 16.

2.3.3 SEM/EDS

Scanning electron microscopy and energy dispersive X-ray spectrometry (SEM/EDS) (SEM SU3500 Oxford EDS EMAX Evolution, Hitachi) was performed to observe the surface of specimen and to collect EDS spectra from silicone rubber and stainless steel. The accelerating voltage was 15kV, and operating pressure was 30Pa.

3 Results

3.1 Friction in various environments

3.1.1 Measurement of friction coefficient

Figure 2 (a)~(c) shows the transition of friction coefficient (COF) of silicone rubber in dry air and hydrogen together with the moisture content. *Figure 2 (d)~(l)* shows enlarged views of (a), (b) and (c), expressing the shape of the friction curves. Moisture contents in hydrogen ranged from 0.4 to 0.9 ppm (hereinafter called dry hydrogen) and from 83 to 110 ppm (humid hydrogen), while that in air (dry air) was from 1.4 to 2.0 ppm.

Comparing the results among the gases which have similar moisture content, the friction coefficients after 2000 seconds in dry hydrogen were higher than those in dry air. Furthermore, the friction coefficients after 2000 seconds in dry hydrogen was higher than those in humid hydrogen.

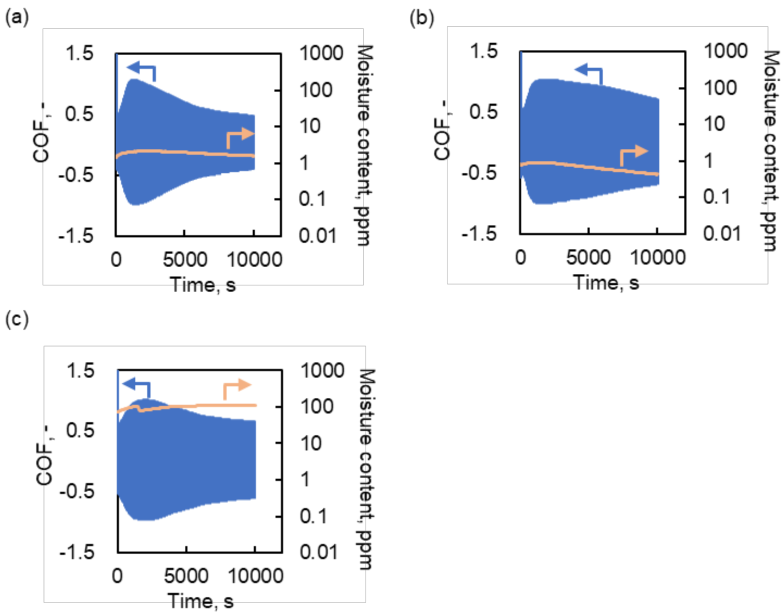

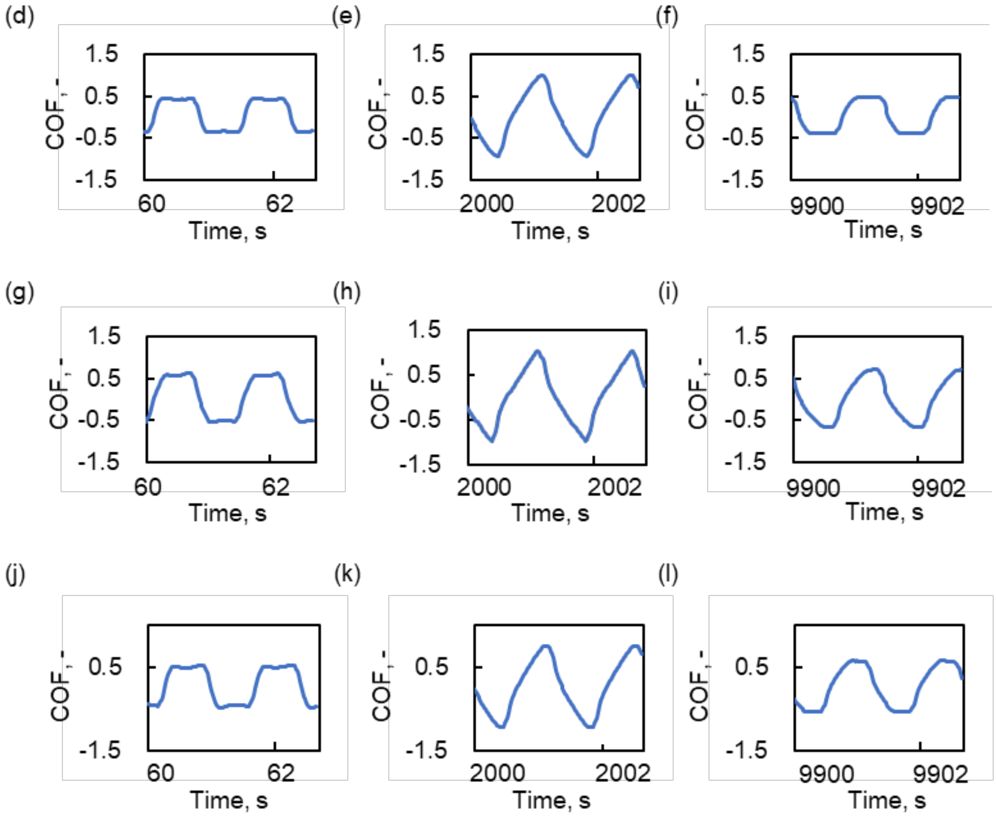

Figure 2: Transition of friction coefficient (a) in dry air, (b) in dry hydrogen, (c) in humid hydrogen, (d)(e)(f) Enlarged view of the result in dry air, (g)(h)(i) Enlarged view of the result in dry hydrogen, (j)(k)(l) Enlarged view of the result in humid hydrogen

The shape of the friction curve also depended on the environment (*Figure 2 (d)~(l)*). After 60 seconds from measurement start, the shape of friction curves was similar among all gases. The shape has plateau region, indicating that the silicone rubber slipped on the surface of stainless steel. The shape changed to a triangular shape after 2000 seconds, which suggests that silicone rubber sticked to stainless steel and did not slip on it. After 9900 seconds, the duration on the plateau region in the friction curve in dry hydrogen was shorter than that in dry air. In addition to that, that in dry hydrogen was shorter than that in humid hydrogen.

3.2 Surface analysis after sliding test

3.2.1 Morphology measurement

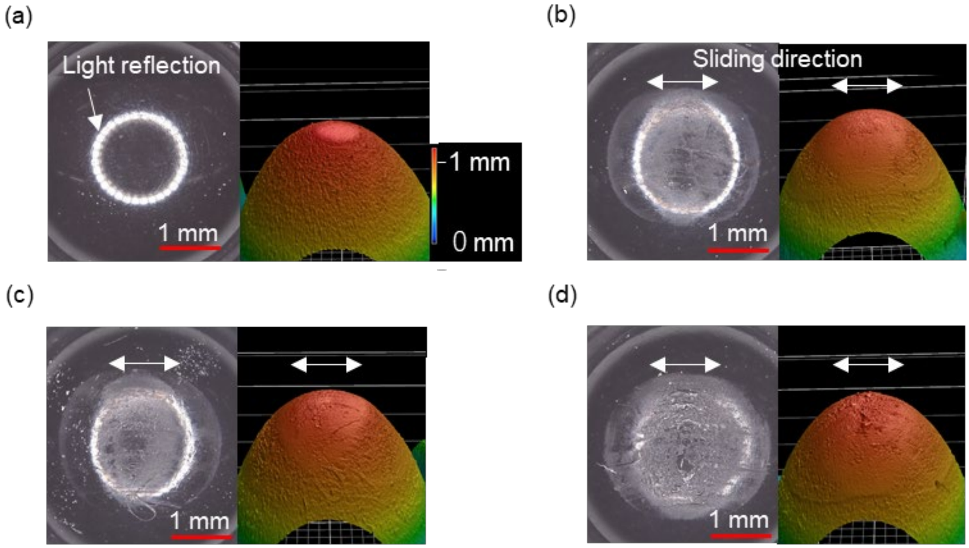

Figure 3: Microscope image and 3D image of (a) virgin rubber before the friction test, (b) rubber after the friction test in dry air, (c) rubber after the friction test in dry hydrogen,(d) rubber after the friction test in humid hydrogen

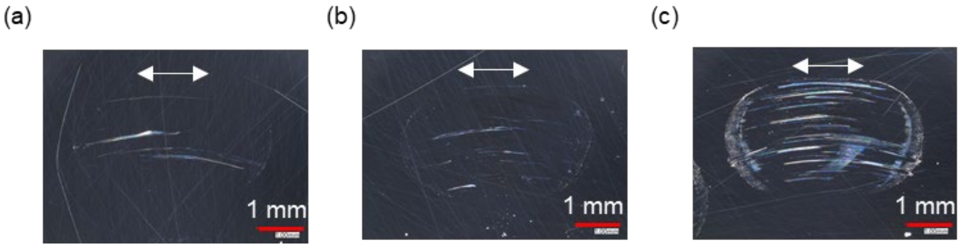

Figure 4: Microscope image of stainless steel after the friction test (a) in dry air (b) in dry hydrogen (c) in humid hydrogen

The microscope images and 3D shape obtained using confocal laser scanning microscopy are shown in *Figure 3*. The rubber surface after the sliding test in humid hydrogen (*d*) showed severe wear compared to that in dry air (*b*) and that in dry hydrogen (*c*). There was no clear difference between the rubber surface after sliding test in dry hydrogen and that in dry air. As shown in *Figure 4*, the stainless steel after sliding test in humid hydrogen exhibited a clear wear track, in addition to the severe wear on the rubber surface.

3.2.2 Investigation of chemical composition change

IR spectra of rubber surface were measured in order to analyse chemical composition changes. The spectra were shown in *Figure 5*. The peaks were observed at 787, 1006, 1258 and 2962 cm^{-1} for silicone polymer and 452 and 1068 cm^{-1} for silica filler. The observed peaks were reasonable because silicone rubber was composed of silicone polymer and silica filler. The IR spectra were normalized at 787 cm^{-1}, which was assigned to Si-C bonds of silicone polymer. The peak intensity at 452 cm^{-1} and at 1068 cm^{-1} increased after sliding tests compared to the spectrum of silicone rubber before sliding test. It suggested that the amount of silicone polymer decreased compared to that of silica filler after sliding test. The amount of silica filler on rubber surface after sliding test in humid hydrogen was greater than that in dry hydrogen. The amount of silica filler on rubber surface after sliding test in dry hydrogen was greater than that in dry air.

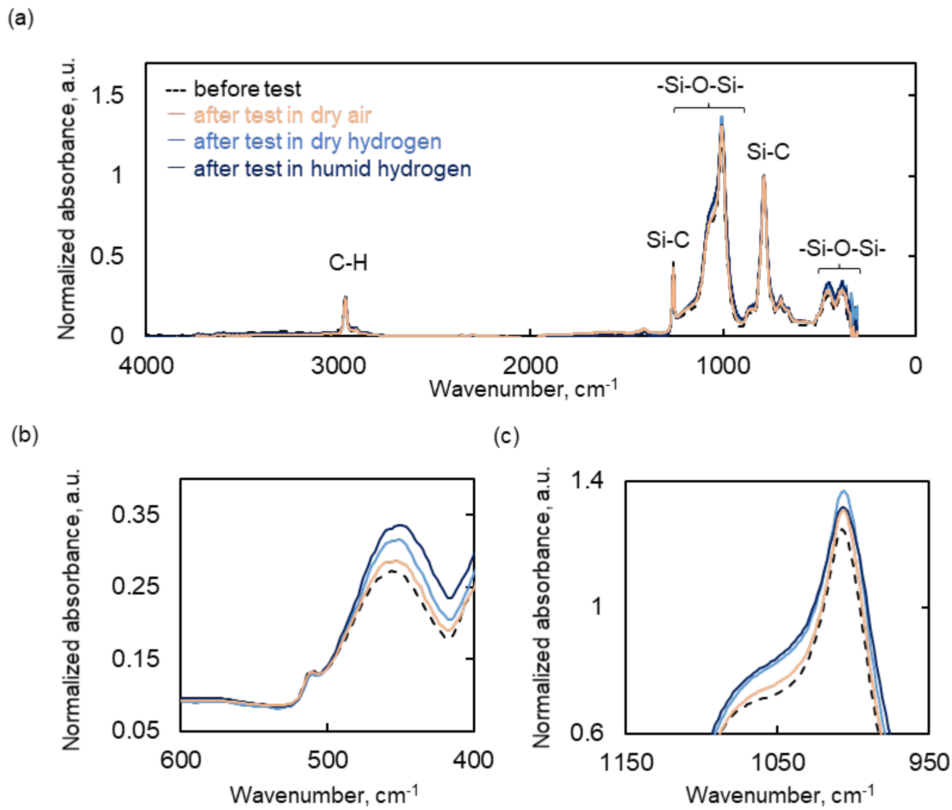

Figure 5: IR spectra of rubber surface normalized at 787 cm^{-1}

Although the observed wear appearance and wear debris were different in degree among the three conditions, the results in FTIR and SEM/EDS were similar.

Therefore, the analysis results for humid hydrogen were particularly shown in *Figure 6*. As shown in *Figure 6(b)*, the IR spectra at the edge of the friction tracks have peaks at 1100, 1258 and 2962 cm^{-1}. The peaks at 1258 and 2962 cm^{-1} were assigned to Si-C and C-H bonds of silicone polymer. The peak at 1100 cm^{-1} was assigned to Si-O-Si bonds of silicone polymer and silica filler. The EDS mapping of silicon also indicated that the particles includes silicon atoms (*Figure 6(c) and (d)*). Thus, debris of silicone rubber were transferred on the stainless steel surface. On the other hand, grooves directed to sliding direction were observed at the centre of the stainless steel (*Figure 6(e)*).

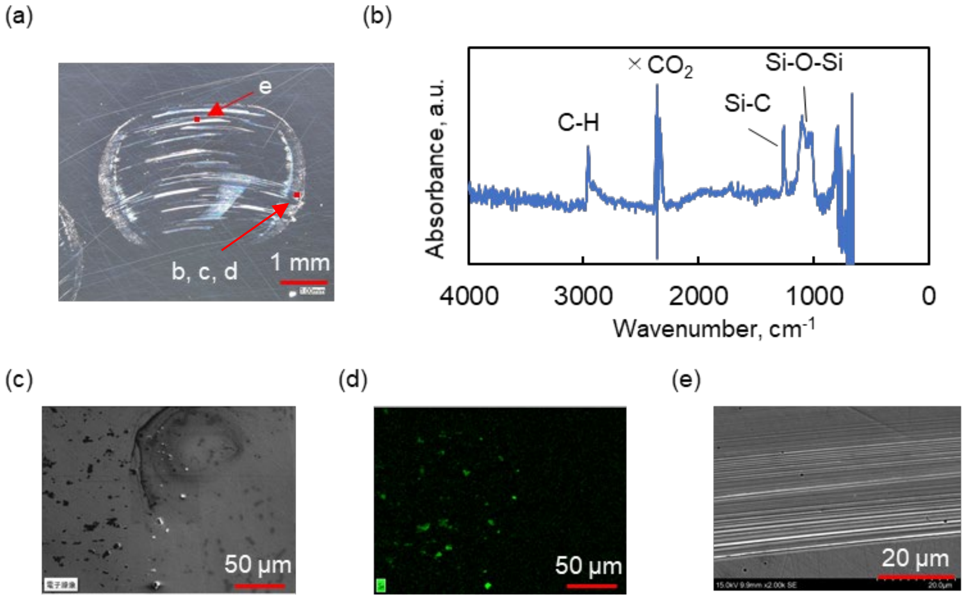

Figure 6: The analysis of countersurface after sliding test in humid hydrogen (a) Microscope image of stainless steel surface after sliding test, (b) IR spectrum obtained from the edge of wear track, (c) SEM image at the edge of wear track, (d) EDS elemental distribution map of silicon atom, (e) SEM image at the centre of wear track

4 Discussion

All the results described above suggest influences of the hydrogen environment and moisture content on the friction behaviour of silicone rubber.

As for the influence of hydrogen, friction coefficients in hydrogen after reaching its peak were higher than that in air at a similar moisture content. After sliding test in dry hydrogen, the amount of silica filler on the rubber surface increased compared to that in dry air. These phenomena may have been caused by the absence of oxidative reaction in hydrogen. When oxidative reaction occurred on rubber surface in dry air, the hardness of rubber surface increase, resulting in lower friction coefficients and reduced exposure of silica filler. However, there are other possibilities, such as the influence of hydrogen to silicone rubber. Further study will be necessary to understand the respective aspects.

Tribological characteristics of the silicone rubber were also sensitive to moisture content. Friction coefficient in dry hydrogen after reaching its peak is higher than that in humid hydrogen. After sliding test in humid hydrogen, the amount of silica filler on the rubber surface increased compared to dry hydrogen. These results may have been caused by hydrolysis reaction of silicone polymer. Similar change in IR spectrum was reported by Nagasawa [23]. Hydrolysis of silicone polymer may enhance the degradation of silicone polymer, resulting in low friction coefficients and increased exposure of silica filler. In another possibility, lower friction coefficients and increased exposure of silica filler in humid hydrogen may have been caused by the time difference in rubber slipping on stainless steel. Further study will be necessary as well.

Deep grooves were observed on the stainless steel after the sliding test in humid hydrogen. These grooves appear to have have been caused by the wear resulting from the exposed silica on the rubber surface.

5 Conclusions

In order to clarify the features of friction in hydrogen, influences of gas and moisture content to friction and wear were investigated.

As for the influence of hydrogen, friction coefficients in hydrogen were higher than those in air at a similar moisture content. Moisture content also influenced friction coefficients. The friction coefficients in the dry condition were higher than those in high humidity conditions. As moisture content increases, silicone polymer was selectively removed from the rubber surface during sliding test. As a result, the silica fillers were exposed on the rubber surface and the groove may have been generated on the stainless steel.

6 Acknowledgements

This research work was performed within the framework of the strategic international collaborative research program (SICORP, grant number: JPMJSC2121), which was supported by Japan Science and Technology Agency (JST), and the joint research project “SusSeal4H2” (funding code: 01DR23001), which was co-funded by German Federal Ministry of Education and Research.

Friction tests were performed at HYDROGENIUS (the Research Center for Hvdrogen Industrial Use and storage) in the Kyushu University.

The authors are grateful to the Bundesanstalt für Materialforschung und -prüfung (BAM), namely Dr. Theiler and Dr. Murillo, to Freudenberg Technology Innovation

SE & Co. KG corporate R&D, namely Dr. Dobbelaar, Dr. Schauber and Mr. Müller for informative discussion.

7 References

[1] Yamabe, J., Nishimura, S.; *Influence of fillers on hydrogen penetration properties and blister fracture of rubber composites for O-ring exposed to high-pressure hydrogen gas,* International Journal of Hydrogen Energy, 2009, https://doi.org/10.1016/j.ijhydene.2008.11.105

[2] Yamabe, J., Nishimura, S., Koga, A.; *A study on sealing behavior of rubber O-ring in high pressure hydrogen gas*, SAE International Journal of Materials and Manufacturing, 2009, https://doi.org/10.4271/2009-01-0999

[3] Yamabe, J., Fujiwara, H., Nishimura, S.; *Fracture analysis of rubber sealing material for high pressure hydrogen vessel*, Journal of Environment and Engineering, 2011, https://doi.org/10.1299/jee.6.53

[4] Fujiwara, H., Yamabe, J., Nishimura, S.*; Evaluation of the change in chemical structure of acrylonitrile butadiene rubber after high-pressure hydrogen exposure,* International Journal of Hydrogen Energy, 2012, https://doi.org/10.1016/j.ijhydene.2012.02.084

[5] Yamabe, J., Koga*,* A., Nishimura, S.; *Failure behavior of rubber O-ring under cyclic exposure to high-pressure hydrogen gas,* Engineering Failure Analysis, 2013, https://doi.org/10.1016/j.engfailanal.2013.01.034

[6] Fujiwara, H., Ono, H., Nishimura, S.; Degradation behavior of acrylonitrile butadiene rubber after cyclic high-pressure hydrogen exposure, International Journal of Hydrogen Energy, 2015, http://dx.doi.org/10.1016/j.ijhydene.2014.11.106

[7] Ono, H., Fujiwara, H., Onoue, K., Nishimura, S.; *Influence of repetitions of the high-pressure hydrogen gas exposure on the internal damage quantity of high-density polyethylene evaluated by transmitted light digital image,* International Journal of Hydrogen Energy, 2019, https://doi.org/10.1016/j.ijhydene.2019.07.035

[8] Fujiwara, H., Ono, H., Onoue, K., Nishimura, S.; *High-pressure gaseous hydrogen permeation test method -property of polymeric materials for high-pressure hydrogen devices (1)-,* International Journal of Hydrogen Energy, 2020, https://doi.org/10.1016/j.ijhydene.2020.07.215

[9] Fujiwara, H., Ono, H., Ohyama, K., Kasai, M., Kaneko, F., Nishimura, S.; *Hydrogen permeation under high pressure conditions and the destruction of exposed polyethylene-property of polymeric materials for high-pressure hydrogen devices (2)-*, International Journal of Hydrogen Energy, 2021, https://doi.org/10.1016/j.ijhydene.2020.12.223

[10] Castagnet, S., Ono, H., Benoit, G., Fujiwara, H., Nishimura, S.; *Swelling measurement during sorption and decompression in a NBR exposed to high-pressure hydrogen*, International Journal of Hydrogen Energy, 2017, https://doi.org/10.1016/j.ijhydene.2017.06.138

[11] Simmons, K.L., Kuang, W., Burton, S.D., Arey, B.W., Shin, Y., Menon, N.C., Smith, D.B., H-Mat; *Hydrogen compatibility of polymers and elastomers,* International Journal of Hydrogen Energy, 2021, https://doi.org/10.1016/j.ijhydene.2020.06.218

[12] Zhou, C., Zheng, J., Gu, C., Zhao, Y., Liu, P.; *Sealing performance analysis of rubber O-ring in high-pressure gaseous hydrogen based on finite element method,* International Journal of Hydrogen Energy, 2017, https://doi.org/10.1016/j.ijhydene.2017.03.039

[13] Zhou, C., Zheng, Y., Liu, X.; *Fretting characteristics of rubber X-ring exposed to high-pressure gaseous hydrogen*, energies, 2022, https://doi.org/10.1016/j.ijhydene.2019.02.224

[14] Zhou, C., Chen, G., Xiao, S., Hua, Z., Gu, C.; *Study on fretting behavior of rubber O-ring seal in high-pressure gaseous hydrogen*, International Journal of Hydrogen Energy, 2019, https://doi.org/10.3390/en15197112

[15] Duranty, E. R., Roosendaal, T. J., Pitman, S. G., Tucker, J. C., Owsley, Jr. S. L., Suter, J. D., Alvine, K. J.: *An in situ tribometer for measuring friction and wear of polymers in a high pressure hydrogen environment*, Review of Scientific Instruments, 2017, https://doi.org/10.1063/1.5001836

[16] Kuang, W., Bennett, W. D., Roosendaal, T. J., Arey, B. W., Dohnalkova, A., Petrossian, G., Simmons, K. L.: *In situ friction and wear behavior of rubber materials incorporating various fillers and/or a plasticizer in high-pressure hydrogen,* Tribology International, 2020, https://doi.org/10.1016/j.triboint.2020.106627

[17] Furusho, K., Tanaka, H., Yagi, K., Sawae, Y., Honda, S.: *9th International Tribology Conference, Fukuoka 2023*, https://confit.atlas.jp/guide/event/itc2023/top, visited on September 30, 2023

[18] Sawae, Y., Morita, T., Takeda, K., Onitsuka, S., Kaneuti, J., Yamaguchi, T., Sugimura, J.: *Friction and wear of PTFE composites with different filler in high purity hydrogen gas,* Tribology International, 2021, https://doi.org/10.1016/j.triboint.2021.106884

[19] Theiler, G., Gradt, T.: *Tribological characteristics of polyimide composites in hydrogen environment,* Tribology International, 2015, https://doi.org/10.1016/j.triboint.2015.06.001

[20] Theiler, G., Gradt, T.: *Environmental effects on the sliding behaviour of PEEK composites,* Wear, 2016, https://doi.org/10.1016/j.wear.2016.09.019

[21] Theiler, G., Gradt, T.: *Influence of counterface and environment on the tribological behaviour of polymer materials*, Polymer Testing, 2021, https://doi.org/10.1016/j.polymertesting.2020.106912

[22] Fukuda, K, Sugimura, J.: *Influences of trace water in a hydrogen environment on the tribological properties of pure iron,* Tribology Online, 2013, https://doi.org/10.2474/trol.8.22

[23] Nagasawa, S., Nishina, H., Arase, N., Nakada, M.: *Simulation test method for deterioration of engine crankshaft oil seals*, SAE International, 1990, https://doi.org/10.4271/902123

8 Authors

NOK corporation

4-3-1 Tsujidoshinmachi Fujisawa-shi, Kanagawa-ken, 251-0042 Japan:

Hikaru Hashimoto, M. Sc., hashimoto.18.hikaru@jp.nokgrp.com

Suguru Norikyo, M. Sc., norikyo.21.suguru@jp.nokgrp.com

Dr.-Eng. Ayako Aoyagi, aoyagi.07.ayako@jp.nokgrp.com

Kyushu University, Faculty of Engineering, Department of Mechanical Engineering

744 Motooka Nishi-ku, Fukuoka-ken, 819-0395 Japan:

Univ.-Asst. Prof. Dr.-Eng. Hiroyoshi Tanaka, ORCID 0000-0002-2392-4789,

tanaka.hiroyoshi.315@m.kyushu-u.ac.jp

Takehiro Morita, M. Sc.,

morita.takehiro.871@m.kyushu-u.ac.jp

Univ.-Prof. Dr.-Eng. Yoshinori Sawae, ORCID 0000-0001-9255-5297,

sawae.yoshinori.134@m.kyushu-u.ac.jp

Dr.-Eng. Joichi Sugimura, ORCID 0000-0003-1926-2169,

sugimura.joichi.666@m.kyushu-u.ac.jp

https://doi.org/10.61319/O2Y6V8UJ